Physica E 43 (2011) 1162–1165

Contents lists available at ScienceDirect

Physica E

journal homepage: www.elsevier.com/locate/physe

Intraband spectroscopy of excited quantum dot levels by measuring photoinduced currents

B. Eichenberg [a,*], S. Dobmann [a], H. Wunderlich [a], A. Seilmeier [a], L.E. Vorobjev [b], D.A. Firsov [b], V. Panevin [b], A.A. Tonkikh [c]

[a] Physikalisches Institut, Universität Bayreuth, Universitätsstrasse 30, 95447 Bayreuth, Germany
[b] St. Petersburg State Polytechnic University, 195251 St. Petersburg, Russia
[c] St. Petersburg Academic University of RAS, 194021 St. Petersburg, Russia

ARTICLE INFO

Article history:
Received 16 August 2010
Accepted 21 January 2011
Available online 28 January 2011

ABSTRACT

The development of semiconductor quantum dot (QD) devices particularly for the infrared requires information on their intraband energy levels. For most of the samples FTIR spectroscopy does not provide reliable results on intraband transitions in the mid-infrared due to very low absorption signals. In recent years photocurrent spectroscopy was demonstrated as an alternative method. In this paper we present a modified photocurrent method, which does not require complicated contact structures or contact layers. The samples are laterally contacted by simply soldering wires and are biased by several 10 V. The intraband resonances are monitored via current changes induced by optical excitation with intense picosecond mid-infrared laser pulses. Both bound to bound and bound to continuum transitions enhance the current. We present data taken on two highly n-doped GaAs/InAs QD samples with different doping concentration at 77 K and at room temperature. In this way, a nearly complete picture of intraband transitions between excited levels in the conduction band is obtained. The intraband spectra obtained with this technique nicely agree with calculated QD intraband levels.

© 2011 Elsevier B.V. All rights reserved.

1. Introduction

In recent years semiconductor quantum dot (QD) structures attracted remarkable interest in fundamental research and for applications due to their favorable optical and electrical properties [1]. Especially semiconductor lasers with low threshold current [2] have been demonstrated and QD photodetectors for the mid-infrared range (MIR) operating at room temperature are under intense investigation [3–6].

In spite of all these successful applications, there is still a lot of basic work to be done to characterize these structures particularly in the MIR. The widely used standard technique for investigating intersubband (ISB) transitions in 2D semiconductor heterostructures or intraband (IB) transitions (also denoted as intersublevel transitions) in QD structures is the Fourier transform infrared (FTIR) spectroscopy. It provides reliable results in 2D systems but fails to resolve IB resonances in most QD structures on account of their moderate absorption cross sections combined with a low dot density resulting in tiny absorption signals. Although intraband absorption is clearly detected in GaN QD samples [7], the intraband absorption of QDs consisting of materials like InAs, which is located in the mid- and far-infrared, is hard to detect [8] in the background noise of the spectrometer.

Another complementary technique for the investigation of intraband transitions in the MIR is the photocurrent spectroscopy, which provides enhanced photocurrent signals subsequent to photoexcitation of IB resonances. The signal strengths depend on the absorption cross section and on the carrier escape probabilities. For such investigations sophisticated contact structures are used: contact layers to apply a voltage perpendicular to the QD layers [9,10], or interdigitated contacts for the application of in-plane fields [11]. Up to now, to our knowledge, only QDs with low doping concentrations have been investigated under low intensity excitation and at cryogenic temperatures. In that papers, only excitations from dot ground states to the wetting layer and to continuum states in the conduction and the valence band [12] were monitored.

In this contribution, we present a photocurrent method for a simple access to intraband levels of QD samples, which does not need sophisticated contacts and which may also be used at ambient temperature. Intense ultrashort laser pulses tunable in the MIR are used to excite intraband transitions in the conduction band of QDs resulting in clear photocurrent signals. The potential of the method is shown with the help of investigations on highly

* Corresponding author. Tel.: +49 921553161; fax: +49 921553172.
E-mail address: boris.eichenberg@uni-bayreuth.de (B. Eichenberg).

1386-9477/$ - see front matter © 2011 Elsevier B.V. All rights reserved.
doi:10.1016/j.physe.2011.01.021

doped InAs QD samples. Experimental data taken on samples with different doping concentrations and at different temperatures give a nearly complete picture of the intraband levels. The results are in good agreement with calculations.

2. Experimental

In the experiments photoinduced current changes due to photoexcitation of intraband transitions in the QDs via ultrashort infrared pulses are measured. The sample geometry with two 45° facets and the electrical circuit used in our experiments are shown in Fig. 1. The samples are contacted by simply fixing gold wires on both sides of the top of the QD layers with pure Indium solder at a temperature of approximately 160 °C. The sample is integrated in an electrical circuit with a series resistor of 10 MΩ, which is connected to a voltage supply adjustable between 0 and 100 V. Intraband transitions of the QDs are photoexcited by intense tunable MIR picosecond pulses that are focused to one of the facets. The MIR pulses of 10 Hz repetition rate are generated via difference frequency generation between the emission of a modelocked Nd:YLF laser and the near-infrared emission of an optical parametric oscillator [13]. The MIR pulses excite electrons resonantly to upper levels, which exhibit higher probability for thermionic emission or tunnel escape, or even transitions to the continuum may take place. In this way the conductivity in the QD layers increases and a photoinduced current is expected that can be detected via the voltage drop at the QD sample with the help of an oscilloscope.

3. The QD samples

To test our method we used GaAs/InAs QD samples grown by the Stranski–Krastanow method on semi-insulating GaAs substrates [14,15]. A 25 nm thick $Al_{0.25}Ga_{0.75}As$/GaAs superlattice is followed by a 240 nm wide GaAs buffer layer. The active region of our samples consists of 30 periods of a dot-in-well structure. Each of them contains a 40 nm GaAs barrier, an InAs wetting layer and the InAs QDs overgrown by a strain reducing layer of $In_{0.12}Ga_{0.88}As$. The GaAs barriers are n-doped in a 2 nm wide region about 1.5 nm below each wetting layer. The doping concentration amounts to $1.5\times10^{18}\,cm^{-3}$ carriers in sample A and $6\times10^{17}\,cm^{-3}$ in sample B. This active region is capped by another 25 nm thick $Al_{0.25}Ga_{0.75}As$/GaAs superlattice and a GaAs cap layer.

The selforganized growth creates islands of pyramidal shape due to the lattice mismatch of InAs and GaAs. During the subsequent overgrowth process, Indium from the strain reducing $In_{0.12}Ga_{0.88}As$ layer diffuses towards the pyramids resulting in QDs with the shape of truncated pyramids. The pyramids have a base length of about 18 nm and a height of around 6 nm as shown in the inset of Fig. 2 [14,15]. In consequence the Indium content of the $In_{0.12}Ga_{0.88}As$ alloy decreases in the direct vicinity of the dots within the diffusion length to approximately zero. Therefore we assume an in plane conduction band scheme as sketched in Fig. 2 in which the QDs are enclosed by GaAs. We prepared a 5 mm long piece of sample A, and a 1 mm long piece of sample B, both with two 45° facets.

First information on intraband transitions is generally expected from FTIR measurements. Best results are generally obtained, taking difference spectra using a reference sample carefully prepared from the pure substrate material with the same geometry. Such spectra did not show any clear resonances due to the low intraband absorption of the QD layers even in sample A with five internal reflections. To suppress signal contributions due to small differences of the samples, we divided FTIR spectra taken at 20 and 300 K (see Fig. 3a), a representation in which only temperature dependent resonances show up. So absorption bands which are more pronounced at room temperature appear as peaks and resonances with increased absorption at 20 K as dips. Beside relatively strong residual absorption lines of H_2O and CO_2, we find a peak at about 96 meV, indicating an increased intraband absorption at 300 K. If we look closer, a broad low temperature resonance dip between 125 and 145 meV suggests an intraband absorption, which is more pronounced at 20 K.

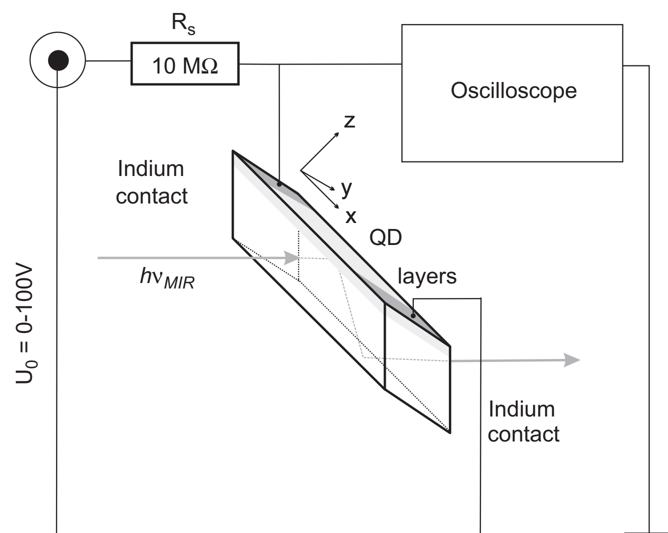

Fig. 1. Experimental setup for the photocurrent measurements. The MIR excitation pulses are focused to a 45° facet and reflected at the QD layers. The subsequent current changes are measured via voltage changes at the QD sample by an oscilloscope.

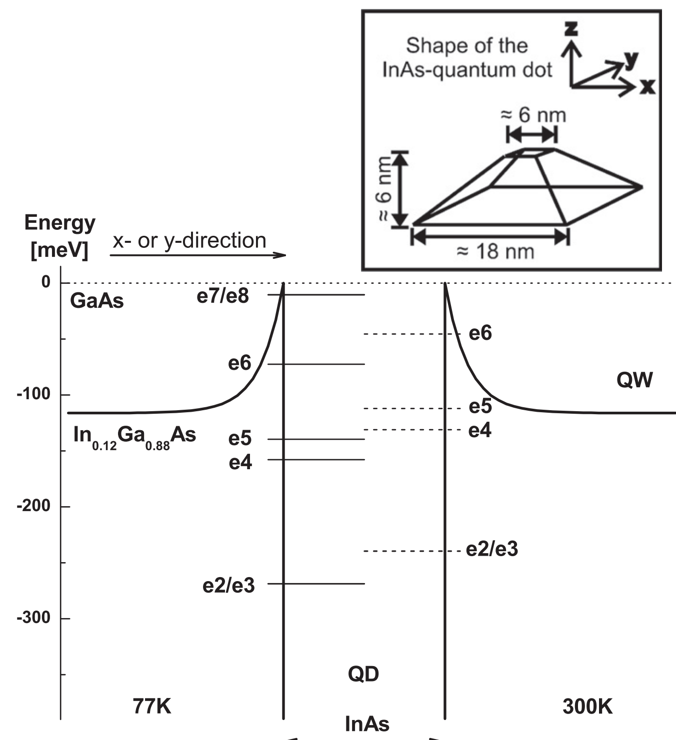

Fig. 2. In plane conduction band structure of the InAs QDs embedded in the strain reducing $In_{0.12}Ga_{0.88}As$ layer. The calculated QD levels are shown for 77 and 300 K. Inset: geometry and size of the QDs.

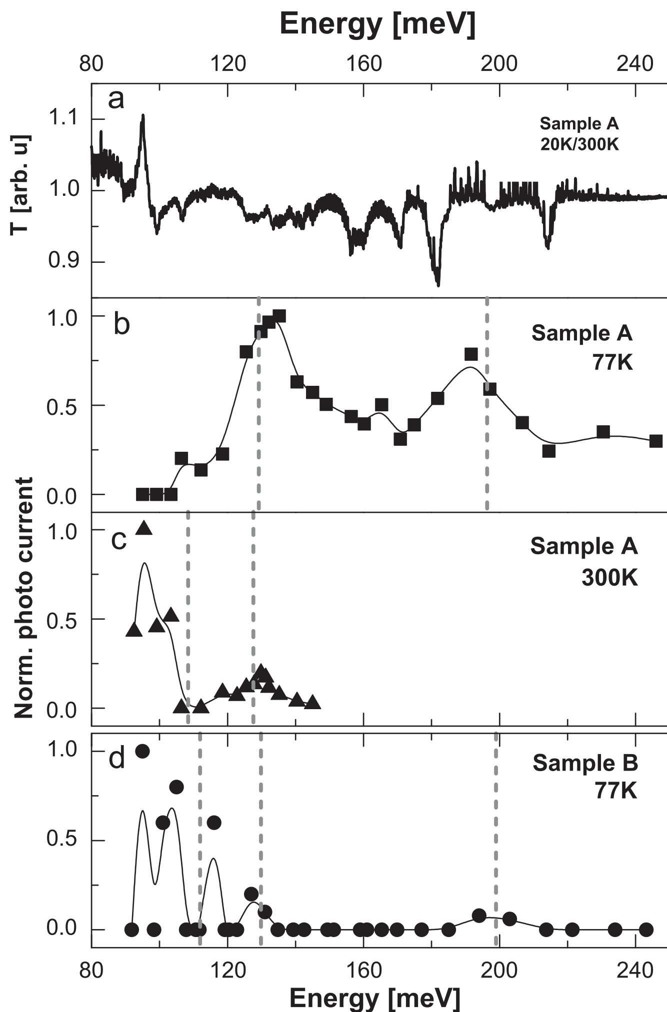

Fig. 3. Intraband spectra of the QDs of sample A (a)–(c) and of sample B (d). (a) Ratio of FTIR transmission spectra taken at 20 and 300 K. Photoinduced current change (b)–(c) of the QD sample A at 77 and 300 K and (d) of sample B at 77 K after intense MIR excitation. The vertical dashed lines indicate calculated transitions.

4. Photocurrent measurements

Data on photoinduced current changes taken at 77 K and at room temperature are presented in Fig. 3b–d for samples A and B. The spectra are normalized to the excitation energy of the MIR pulses. An excitation of intraband resonances by an intense MIR pulse leads to a voltage signal in the order of 1 mV and a decay time of a few hundred ns, which is determined by the electrical circuit.

Fig. 3b shows the photocurrent changes as a function of the excitation frequency taken at 77 K on sample A (bias voltage 60 V). Here the signals are relatively large, since we used a relatively long sample which allowed five reflections of the MIR beam at the active surface. Broad resonances at about 130 and 190 meV are obvious and an increased background signal is found at frequencies above 130 meV. It should be mentioned that the spectral width of the excitation pulses (2 meV) is narrower than the width of the resonances. From the excitation energy of a few hundred nJ we estimate a maximum sensitivity in the order of 1 A/J.

Fig. 3c presents experimental data taken at 300 K (sample A). Here the bias voltage was only 15 V to prevent damage of the sample, which shows a considerably lower resistance at higher temperatures. FTIR absorption spectra (see above) indicate a clear room temperature resonance below 100 meV. So we focused on that spectral region, in which we find a pronounced photocurrent signal at 95 meV and a small resonance at 130 meV.

Experimental data taken on the second sample B at 77 K are shown in Fig. 3d. The structure of both samples is nearly identical, only the doping concentration is lower in sample B ($n=6\times10^{17}\,\mathrm{cm}^{-3}$). Beyond that, sample B is shorter allowing only a single reflection of the excitation beam at the surface with the QDs. Consequently, the expected photocurrent signals are considerably lower despite of a higher bias voltage of 100 V. In the figure, we observe photocurrent resonances around 100 meV and weaker resonances at 130 and 190 meV. Due to the fact, that both samples have very similar properties, it is not surprising that the frequency positions of the resonances are similar in both samples.

5. Discussion

The photoexcitation of the quantum dots involves transitions between bound states or bound to continuum transitions. If charge carriers are excited to continuum states an increase of the current is evident [5,16]. Moreover, transitions to upper bound QD states may result in a photoinduced current [6,17]. Increased thermionic escape rates due to the lower energy barrier and higher tunneling rates into the wetting layer, or the strain reducing $In_{0.12}Ga_{0.88}As$ layer may contribute to the lateral current [3,18]. An increase of the tunneling rates through the QD barriers due to the relatively weak applied electric field, which never exceeded 500 V/cm, is not expected.

For a more detailed interpretation of the spectra in Fig. 3 calculations of the energy positions of the intraband states of the QDs have to be done. From that results, intraband transition frequencies and their corresponding oscillator strengths are determined. For the special type of QD samples investigated here, there exist highly involved calculations [8,19], based on a full 8×8 $k\cdot p$ theory for modeling the valence and conduction band, which takes into account strain, piezoelectricity and spin orbit coupling. These calculations were made for a smaller QD with a different doping concentration and only for cryogenic temperatures. Moreover, it was assumed that the QD is directly surrounded by GaAs neglecting an In gradient of the strain reducing layer. Therefore, we performed additional calculations for the conduction band using the size and shape of the InAs QDs as shown in Fig. 2 and assuming an In gradient in the vicinity of the QDs as depicted in the figure. For this numerical simulation we used the program Nextnano[3] [20]. To keep computation time in an acceptable range we neglected the coupling of different bands and we assumed that the elastic strain is reduced to a negligible value by the strain reducing layer. Numerical calculations within the framework of this model lead to an unexpected large dot depth followed by a transition energy of $e1\rightarrow e2$ of $\sim$140 meV. However, the positions of the upper energy levels are strongly affected by the energy of the strain reducing layer. Therefore the transitions close to the confinement barriers fit quite well to the experimental data. In Fig. 2 the bound states relevant for the interpretation are inserted as solid and dashed lines for 77 and 300 K, respectively. The calculated electronic intraband transitions between excited levels with an oscillator strength larger than 0.1 are listed in Table 1.

We start with a discussion of the photocurrent spectrum in Fig. 3b taken on sample A at 77 K. We have to keep in mind that each QD is filled with 10 electrons due to the high doping concentration, i.e. the first 5 levels are occupied. A calculation taking into account the Fermi distribution at 77 K shows a complete occupation of levels e1–e4 and an occupation density

Table 1
Calculated energies of intraband transitions of the QD samples at 300 and at 77 K relevant for the interpretation of the photocurrent data.

Transition i→f	Energy (meV) for 300 K	Energy (meV) for 77 K
e2/e3→e4	108	111
e2/e3→e5	128	129
e2/e3→e6	194	196
e4→e7/e8	147	147
e5→e7/e8	128	129

of 90% for level e5. (The Fermi level is pinned by the strain reducing $In_{0.12}Ga_{0.88}As$ layers.) Consequently, efficient intraband photoexcitation is only expected between one of the levels e1–e5 and levels e6 or higher.

The broad resonance at ~130 meV in Fig. 3b is assigned to the transition e5→e7/e8 (see Fig. 2 and Table 1). At excitation frequencies above 130 meV we find an increased photoconduction signal due to carriers excited from e4 and e5 to continuum states, which strongly contribute to the current increase. In that frequency region, another pronounced photocurrent resonance at around 190 meV is detected, which is interpreted as transitions from the occupied e2/e3 states to the unoccupied e6 state with a subsequent escape from the QDs.

Fig. 3c presents the low frequency part of the photoconductivity signal for sample A measured at 300 K. This spectral range is of particular interest, since the FTIR spectrum in Fig. 3a indicates a photocurrent signal at room temperature in contrast to low temperatures. At room temperature the electronic levels e1–e3 are completely filled, the occupancy of level e4 is 70% and that of level e5 is 50%. The occupation of higher levels can be neglected. These numbers show that an absorption from e2/e3 to e4 may be observed at ~100 meV. Indeed we find a strong resonance at this frequency at 300 K in Fig. 3c while at 77 K in Fig. 3b that resonance does not show up due to Pauli Blocking. This finding is in agreement with the result from the FTIR measurements (Fig. 3a). At ~130 meV the e2/e3→e5 and e5→e7/e8 resonances contribute to the signal. The later one is highly pronounced at 77 K (Fig. 3b).

Of special interest is a comparison with the data in Fig. 3d taken on sample B with a lower doping concentration. Numerical calculations give transition frequencies that are within a few meV the same as those presented in Table 1. In sample B each QD contains only ~4 electrons resulting in a sublevel occupation of 100% for level e1 and 50% for the two degenerated levels e2/e3 for 77 K. The other levels are unoccupied.

In Fig. 3d we find a high photocurrent signal at about 100 meV, which corresponds to the transition from occupied e2/e3 levels to the empty e4 level, similar to the situation in sample A at room temperature. As mentioned above, the overall signals from sample B are lower than from sample A, so the accuracy is only limited. However, there is some indication for a splitting of the resonance into two due to a breakup of the degeneracy of levels e2 and e3 caused by strain or the piezoelectric effect [21]. The next resonance at 116 meV might be due to transitions from e2/e3 to the bound state of the wetting layer. This is consistent with calculations for a wetting layer of 3 monolayers thickness. Transitions to this state result in an increased photoconductivity [3]. In Fig. 3b a shoulder at this frequency is also observed. The signal close to 130 meV is attributed to the e2/e3→e5 transition and the signal around 195 meV is interpreted as the e2/e3→e6 transition. Both maxima are observed in sample A, too. The transition e1→e2/e3 does not show up in this experiment, because of the low escape probability of electrons in the confined states e2 and e3. Transitions to continuum states are not detected in sample B, since energies beyond our accessible frequency range are required for transitions from the highest occupied level e3 to the continuum.

6. Conclusion

The experimental investigation of intraband transitions in QDs is still a challenge in most samples. The data presented in the paper show that the detection of photoinduced current changes after intraband excitation with intense ultrashort MIR pulses is a technique, which provides reliable information on intraband transitions despite of their low absorption strengths. The strong MIR excitation allows investigations with simple electrical contacts. From measurements in samples with different doping concentrations and at different temperatures not only transitions from the lowest levels but nearly the complete manifold of the intraband levels is obtained. However, the interpretation of the amplitude of the photocurrent signals is more involved. If the MIR pulse excites the carriers to continuum states we find an absorption edge with an increased current signal at higher energies. Transitions between bound states give rise to absorption bands. In this case, the amplitude of the current signal is not a direct measure of the absorption strength; it depends on the escape probability from the QD, too.

References

[1] D. Bimberg, Semiconductor Nanostructures, Springer, Berlin, 2008.
[2] M. Grundmann, Nano-Optoelectronics: Concepts, Physics and Devices, Springer, Berlin, 2002.
[3] A. Vardi, N. Akopian, G. Bahir, L. Doyennette, M. Tchernycheva, L. Nevou, F.H. Julien, F. Guillot, E. Monroy, Appl. Phys. Lett. 88 (2006) 143101.
[4] Eui-Tae Kim, Anupam Madhukar, Zhengmao Ye, Joe C. Campbell, Appl. Phys. Lett. 84 (2004) 3277.
[5] G. Ariyawansa, A.G.U. Perera, G. Huang, P. Bhattacharya, Appl. Phys. Lett. 94 (2009) 131109.
[6] J. Jiang, S. Tsao, T. O'Sullivan, W. Zhang, H. Lim, T. Sills, K. Mi, M. Razeghi, G.J. Brown, M.Z. Tidrow, Appl. Phys. Lett. 84 (2004) 2166.
[7] Kh. Moumanis, A. Helman, F. Fossard, M. Tchernycheva, A. Lusson, F.H. Julien, B. Damilano, N. Grandjean, J. Massies, Appl. Phys. Lett. 82 (2003) 868.
[8] L.E. Vorobjev, D.A. Firsov, V.A. Shalygin, N.K. Fedosov, V.Yu. Panevin, A. Andreev, V.M. Ustinov, G.E. Cirlin, V.A. Egorov, A.A. Tonkikh, F. Fossard, M. Tchernycheva, Kh. Moumanis, F.H. Julien, S. Hanna, A. Seilmeier, H. Sigg, Semicond. Sci. Technol. 21 (2006) 1341.
[9] A.M. Adawi, E.A. Zibik, L.R. Wilson, A. Lemaitre, J.W. Cockburn, M.S. Skolnick, M. Hopkinson, G. Hill, Appl. Phys. Lett. 83 (2003) 602.
[10] S. Sauvage, P. Boucaud, T. Brunhes, V. Immer, E. Finkman, J.-M. Gerard, Appl. Phys. Lett. 78 (2001) 2327.
[11] L. Chu, A. Zrenner, G. Böhm, G. Abstreiter, Appl. Phys. Lett. 76 (2000) 1944.
[12] E.A. Zibik, A.M. Adawi, L.R. Wilson, A. Lemaitre, J.W. Cockburn, M. Hopkinson, G. Hill, J. Appl. Phys. 100 (2006) 013106.
[13] R. Laenen, K. Wolfrum, A. Seilmeier, A. Laubereau, J. Opt. Soc. Am. B 10 (1993) 2151.
[14] M.V. Maximov, A.F. Tsatsul'nikov, B.V. Volovik, D.S. Sizov, Yu.M. Shernyakov, I.N. Kaiander, A.E. Zhukov, A.R. Kovsh, S.S. Mikhrin, V.M. Ustinov, Zh.I. Alferov, R. Heitz, V.A. Shchukin, N.N. Ledentsov, D. Bimberg, Yu.G. Musikhin, W. Neumann, Phys. Rev. B 62 (2000) 16671.
[15] F. Guffarth, R. Heitz, A. Schliwa, O. Stier, A.R. Kovsh, V. Ustinov, N.N. Ledentsov, D. Bimberg, Phys. Status Solidi (b) 224 (1) (2001) 61.
[16] S.-W. Lee, K. Hirakawa, Y. Shimada, Appl. Phys. Lett. 75 (1999) 1428.
[17] H.P. Porte, P. Uhd Jepsen, N. Daghestani, E.U. Rafailov, D. Turchinovich, Appl. Phys. Lett. 94 (2009) 262104.
[18] H. Lim, W. Zhang, S. Tsao, T. Sills, J. Szafraniec, K. Mi, B. Movaghar, M. Razeghi, Phys. Rev. B 72 (2005) 085332.
[19] L.E. Vorobjev, N.K. Fedosov, V.Yu. Panevin, D.A. Firsov, V.A. Shalygin, M.I. Grozina, A. Andreev, V.M. Ustinov, I.S. Tarasov, N.A. Pikhtin, Yu.B. Samsonenko, A.A. Tonkikh, G.E. Cirlin, V.A. Egorov, F.H. Julien, F. Fossard, A. Helman, Kh. Moumanis, Semicond. Sci. Technol. 22 (2007) 814.
[20] S. Birner, T. Zibold, T. Andlauer, T. Kubis, M. Sabathil, A. Trellakis, P. Vogl, IEEE Trans. Electron Devices 54 (2007) 2137.
[21] M. Grundmann, O. Stier, D. Bimberg, Phys. Rev. B 52 (1995) 11969.